Available online at www.sciencedirect.com

ScienceDirect

Procedia Engineering 207 (2017) 1427–1432

Procedia Engineering

www.elsevier.com/locate/procedia

International Conference on the Technology of Plasticity, ICTP 2017, 17-22 September 2017, Cambridge, United Kingdom

Compressive Behaviours of Raw and Cased Porous Magnesium-alloys determined by X-ray CT

L. C. Chan[a]*, X. Z. Lu[a], C. P. Lai[a], L. W. P. Chow[a]

[a]*Department of Industrial and Systems Engineering, The Hong Kong Polytechnic University, Hung Hom, Kowloon, Hong Kong*

Abstract

Raw porous magnesium-alloys (Mg-alloys) exhibit lightweight properties and crashworthiness, and are widely used in aerospace and transportation industries. However, they have relatively low strength, and are difficult in controlling dimensional accuracy and surface finish. Cased porous Mg-alloys are therefore a potential solution to overcome these drawbacks. In this study, compression tests and X-ray computed tomography (CT) were performed to acquire mechanical properties and investigate structural deformation/fracture behaviours of the specimens, respectively, under different deformation stages. Results indicated that the raw porous Mg-alloy demonstrated good compressibility. Gradual collapse of the pores led a long plastic plateau stress state, which improved the energy absorption and vibration damping abilities. For the cased porous Mg-alloy, initial cracking of the case was observed at 8.5% strain, whereas the porous structure inside seemed unaffected. This indicated that the solid case acted as a functional layer to provide further protection and decoration of the porous structure. In addition, the yield strength and Young's modulus of the cased porous Mg-alloys are able to be controlled and relatively improved, subjected to the variation in case thickness when compared to the constant values of the raw porous Mg-alloy. Thus, this study leads to a benchmark for further research and development on material deformation and failure models of porous Mg-alloys. Meanwhile, engineers would be able to design and customize the porous structure of Mg-alloys efficiently in potential applications such as protective gears and auto-body structures.

Peer-review under responsibility of the scientific committee of the International Conference on the Technology of Plasticity.

* L.C. Chan. Tel.: +852-2766-6634; fax: +852-2362-5267.
E-mail address: lc.chan@polyu.edu.hk

1877-7058 © 2017 The Authors. Published by Elsevier Ltd.
Peer-review under responsibility of the scientific committee of the International Conference on the Technology of Plasticity.
10.1016/j.proeng.2017.10.908

Keywords: Non-destructive; X-ray CT; Porous Structure; Magnesium-alloys

1. Introduction

Porous metal structures have received increased research interests due to their improved functionalities over solid materials [1,2]. A lightweight design with high damping capacity is particularly useful in the aerospace and transportation industries to achieve better mechanical properties and cost reduction. Porous metal structures of aluminium and titanium have been extensively characterized, but there is still a large scope to be explored for porous magnesium [3,4]. Since magnesium has a lower density than aluminium, porous magnesium is regarded as a super lightweight structure. The excellent damping capacity of porous magnesium arises from high frequency resonant vibration modes being excited when an impact force was applied [5]. However, porous structures have low tensile strengths, and defects in the cell walls causes crack formation as stress was concentrated in those areas when loaded [3]. To overcome these drawbacks, porous Mg-alloys fitted with a case appear to be a potential solution. A solid case would improve the yield strength and crashworthiness of the porous structure. This combined structure enables high level of energy absorption through deformation of the porous core and increased strength through the solid casing. Potential applications include aircraft components such as rotor blades and shock absorbers of automobiles.

X-ray CT enables non-destructive investigation of samples internally and externally, and is particularly useful in examining the deformation of pores at increasing compression stages. Studies have been performed using this technique to reveal the correlation between structural and mechanical properties of raw porous structures [6-9], yet the use of X-ray CT to study mechanical behaviours of cased porous structures is limited.

In this study, uniaxial compression tests of raw and cased porous Mg-alloys were carried out at different compression stages, followed by X-ray CT scanning. Dimensional changes were measured and mechanical properties, such as yield strength, initial and effective Young's modulus, were obtained from compression tests. The porous structural transformations at different compression stages were investigated and analysed from the X-ray CT images. As a result, structural changes of the raw and cased porous Mg-alloys under different loading stages and their influence on mechanical properties were presented.

2. Materials and Methods

2.1. Materials and specimens

Porous Mg-alloy specimens were fabricated by a specific infiltration method with a water-soluble space holder. The specimens were wire-cut into Ø 5.5 mm × 10 mm and Ø 4.7 mm × 10 mm, respectively for the raw and cased porous structures. The latter was inserted into a case of the same material with 5.5 mm outer diameter and 0.4 mm thickness. Pore sizes (0.8 mm to 1 mm) and porosity (60% to 75%) of the specimens were controlled by space holders. Protective gas was applied to prevent oxidation and to provide an external pressure to drive the molten metal towards the custom-made space holders, and the specimens were then thoroughly laundered.

2.2. Uniaxial compression tests and X-ray CT tests

Uniaixal compression tests were carried out on a MTS 810 testing machine according to the standard ASTM E9-09. Compressive loading was applied on the specimen and increased until the strain reached a pause value of 5%, the specimen was then unloaded for X-ray CT test. The experiment was repeated for every 5% strain interval until 20% strain. Loading stages of the compression tests were speed-controlled at 0.1 mm/min, while the unloading stages were force-controlled (force rate = -0.1 KN/s). Stress-strain curves of the specimens were recorded and the yield stress and initial Young's modulus were obtained from the 0-5% strain interval. Curves of the unloading stages were fitted to obtain tangent lines, and the gradients were used to calculate the effective Young's moduli.

High-resolution X-ray CT System YXLON FF35 CT was used to carry out X-ray CT tests at 110 kV tube voltage and 100 µA tube current. 720 projections were generated in a 360° rotation, and three-dimensional (3D) volume elements were reconstructed using an in-house reconstruction software, CERA. By defining the relative pixel intensities of the background and material, the surface of the material was determined to obtain the profile and porous structure of the specimen.

3. Results and Discussion

3.1. Dimensional changes of the specimens

As the strain increased, the specimen length of the raw porous Mg-alloy decreased and the diameter increased (Fig. 1a–e, Table 1). After an applied strain of 20%, the length decreased by 22.6% and the diameter increased by 11.9%. The decrease in length is directly proportional to the strain applied, with a decrease of approximately 0.5 mm for every 5% strain. From Fig. 1(e), it could be seen from the specimen shape that there were two indentations, one on each side of the specimen at approximately 45 degrees to each other. This observation suggested that failure of the raw porous Mg-alloy would occur at these points of indentation at a band angle of 45 degrees if the specimen was further compressed, which is in agreement with a previous study [10].

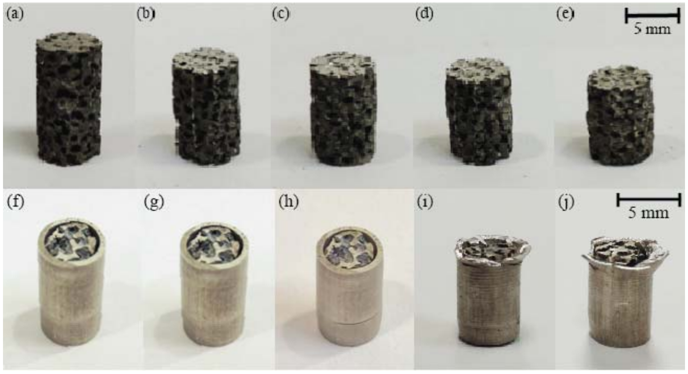

Fig. 1. Topography of the raw porous Mg-alloy at (a) 0%, (b) 5%, (c) 10%, (d) 15%, (e) 20% strain and cased porous Mg-alloy at (f) 0%, (g) 5%, (h) 8.5%, (i) 10% and (j) 15% strain

Table 1 Length and diameter of the raw and cased porous Mg-alloys at different strain levels

Strain (%)	Raw porous Mg-alloy		Cased porous Mg-alloy	
	Length (mm)	Diameter (mm)	Length (mm)	Diameter (mm)
0	10.0	5.54	10.0	5.50
5	9.23	5.65	9.33	5.60
8.5	N/A	N/A	9.02	5.69
10	8.76	5.90	8.97	5.66
15	8.29	5.95	8.42	5.77
20	7.74	6.20	N/A	N/A

Dimensional changes of the cased porous Mg-alloy had a similar trend to that of the raw alloy, but at a slower rate (Fig. 1f–j, Table 1). The length decreased by 15.8% and diameter increased by 4.9% after a 15% strain. Deformation initially occurred at the top of the case, with the porous structure appeared to be unaffected. This suggested that the solid case acts as a protective layer for the porous structure, and after the case was cracked, the porous magnesium inside the case experienced similar compressive behavior as the raw porous Mg-alloy.

3.2. Mechanical properties

The stress-strain and force-deformation curves of the raw and cased porous Mg-alloys were shown in Fig. 2(a) and (b) respectively. The raw porous Mg-alloy was steadily compressed until 20% strain. When the yield stress was reached, the porous Mg-alloy would undergo plastic deformation and collapse of internal pores would give the material good compressibility, energy absorption and vibration damping. However, the cased porous Mg-alloy specimen could only be steadily compressed until 8.5% strain, there was then a sudden decrease in stress accompanied by cracking of the case at the top of the specimen, which indicated the brittle fracture of the Mg case. After that, the case was no longer protective and the porous Mg would endure the compressive loading. As shown in Fig. 2(b), deformation of the raw structure was significantly increased when the applied force was greater than 100 N, and it can withstand a maximum loading of about 1500 N, which implied that the raw structure has the ability to absorb energy by producing large deformation under loading. For the cased structure, only 0.4 mm deformation was measured under a loading of 1500 N, and it could further sustain a loading up to 2400 N, which indicated that the cased structure would be able to withstand a higher compression force than the raw porous structure. Results suggested that the different structures would serve for different applications.

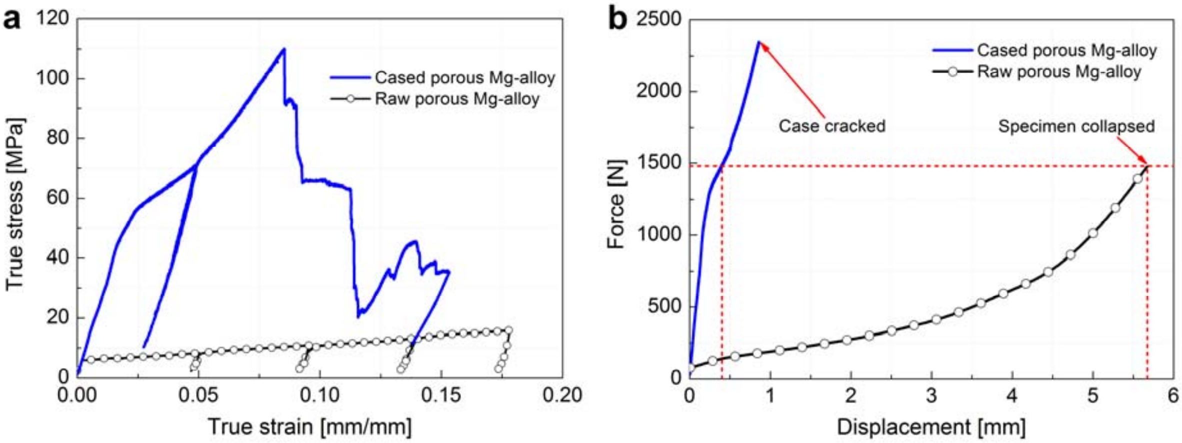

Fig. 2. (a) Stress-strain curves; and (b) force-deformation curves of the raw and cased porous Mg-alloys

Mechanical properties such as yield strength, initial and effective Young's modulus were obtained from the stress-strain curves. As listed in Table 2, the yield strength of the cased porous Mg-alloy was significantly improved compared to the raw one, i.e. from 5.9 MPa to 55.2 MPa. The Young's modulus of the cased porous Mg-alloy was also higher than that of raw one. A rapid drop of true stress occurred after 8.5% strain as the case started to deform and crack tips were formed at the top of the case under subsequent loading. Initial cracks growth along the shear direction were observed between 8.5-10% strain and as a result, the effective Young's modulus was unable to be computed at this stage. The Young's modulus of the cased porous Mg-alloy was decreased to 1.55 GPa when 15% strain was applied, which was similar to the initial Young's modulus of the raw one. In other words, the case's protective effect became negligible and mechanical properties were governed by the inner raw porous structure.

Table 2 Mechanical properties of the raw and cased porous Mg-alloys

		Raw porous Mg-alloy	Cased porous Mg-alloy
Yield strength (MPa)		5.90	55.2
Initial Young's modulus (GPa)		1.46	2.58
Effective Young's modulus (GPa)	Strain level: 5%	2.21	2.85
	Strain level: 10%	2.80	/
	Strain level: 15%	3.44	1.55
	Strain level: 20%	4.24	N/A

3.3. X-ray CT analysis

From X-ray CT image analysis, the average pore size became smaller as the raw porous specimen was compressed (Table 3). It was observed that the shape of the pores was close to spherical initially, then gradually transformed into an ovoid as the specimen was compressed, with the longer axis of the ovoid perpendicular to the loading direction (Fig. 3). The phenomenon was mainly concentrated in the middle of the specimen instead of the top and bottom, which is similar to the typical deformation behavior of metallic porous structures [11]. It was also observed that at 20% strain, the pore boundaries collapsed and the pores became densified in the compression direction, which caused a slight increase in the average pore size (Fig. 3e, Table 3).

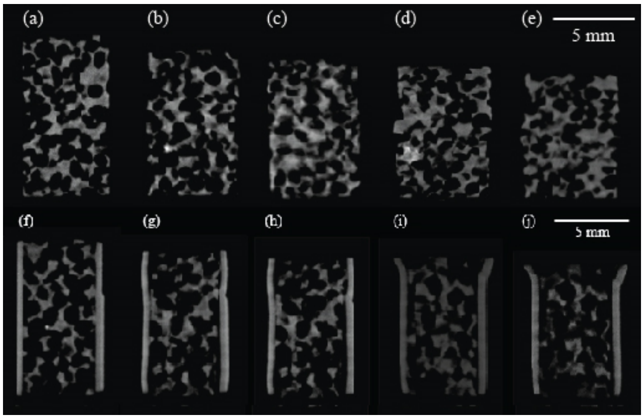

Fig. 3. X-ray CT images of the raw porous specimen at (a) 0%, (b) 5%, (c) 10%, (d) 15%, (e) 20% strain and cased porous Mg-alloy at (f) 0%, (g) 5%, (h) 8.5%, (i) 10% and (j) 15% strain

Table 3 Average pore size of the raw and cased porous specimen at different strain rates

Strain (%)	Raw porous Mg-alloy (mm)	Cased porous Mg-alloy (mm)
0	1.01	1.02
5	0.88	1.00
8.5	N/A	0.91
10	0.76	1.01
15	0.76	0.91
20	0.79	N/A

For the cased porous Mg-alloy, it could be seen that the length was reduced for both the porous structure and the case before a strain level of 8.5%. As the case cracked at 8.5% strain, the top of the case expanded outwards on both sides and the porous structure appeared to be unaffected. Analysis of the X-ray CT images indicated that the average pore size of the porous structure remained almost constant throughout the compression, suggesting that the majority of the stress from the compression was applied to the case instead of the porous structure, and hence the case cracked before the inner porous structure deform. After 8.5% strain, the porous structure began to be compressed as indicated by the sharp decrease in stress in Fig. 2 (refer to section 3.2).

4. Conclusions

The compressive properties of raw and cased porous Mg-alloys and structural transformation at different compression stages were determined by X-ray CT. Results are summarised as follow:

1. The raw porous Mg-alloy was able to absorb impact energy and deform without failure, and the collapse of internal pores gave the material good compressibility, energy absorption and vibration damping. For the cased porous Mg-alloy, initial cracking of the case was observed at 8.5% strain, whereas the porous structure inside seemed unaffected. This implied that the internal porous structure could be protected by a case of certain thickness. In addition, the yield strength and initial Young's modulus of the cased porous Mg-alloy was significantly improved compared to the raw porous Mg-alloy.
2. The average pore size and transformation of porous morphology at different compressive stages were measured with the aid of X-ray CT. The case acted as a protective layer for the inner porous structure and limited pores dislocation or collapse occurred when an external force was applied, until the case cracked at 8.5% strain. Gradual evolution of the porous structure under compressive loading of the raw porous Mg-alloys was observed. X-ray CT enabled investigation of the whole deformation phenomena and record geometric changes of pores during compression.

However, the above conclusions could only be made for compression strain up to 20%. The cased structure would be able to withstand a higher compression force than the raw porous structure, hence it would be useful in applications where structural strength is needed. In order to gain further understanding of the interactions between the case and porous core, it is recommended to study cases with various thicknesses and other materials with good ductility for the casing to observe their deformation behaviours. A separate project is currently underway to investigate the mechanical properties, fracture mechanism and energy absorption of both raw and cased porous Mg-alloys structures under different transformation stages such as collapse and densification. In addition, this study provided a benchmark for further research and development on material deformation and failure models for porous Mg-alloys. It will allow engineers to design and customise porous structures of Mg-alloys with different case thicknesses efficiently in potential applications such as protective gears and auto-body structures.

Acknowledgements

The work described in this paper was partially supported by the Research Committee of the Hong Kong Polytechnic University (Project No. G-YBRL and G-YL64) and Large Equipment Fund of the Hong Kong Polytechnic University (Project No. DD6X).

References

[1] J.H. Qin, Q. Chen, C.Y. Yang, Y. Huang, Research process on property and application on metal porous materials, J. Alloy Compd., 654 (2016) 39-44.
[2] K.A. Dannemann, J. Lankford, High strain rate compression of closed-cell aluminium foams, Mater. Sci. Eng.: A, 293 (2000) 157-164.
[3] H. Cay, H. Xu, Q. Li, Mechanical behavior of porous magnesium/alumina composites with high strength and low density, Mat. Sci. Eng. A, 574 (2013) 137-142.
[4] C.E. Wen, Y. Yamada, K. Shimojima, Y. Chino, H. Hosokawa, M. Mabuchi, Compressibility of porous magnesium foam: dependency on porosity and pore size, Mater. Lett., 58 (2004) 357.
[5] Z.K. Xie, M. Tane, S.K. Hyun, Y. Okuda, H.Nakajima, Vibration-damping capacity of lotus-type porous magnesium, Mater. Sci. Eng. A, 417 (2006) 129–133.
[6] A. Vahidgolpayegani, C. Wen, P. Hodgson, Y. Li, 2 – Production methods and characterization of porous Mg and Mg alloys for biomedical applications, in: C.Wen, Metallic Foam Bone: Processing, Modification and Characterization and Properties, Woodhead Publishing, Cambridge, 2016, pp. 25–82.
[7] M. Ahn, J. Lee, Y. Koh, Rapid direct deposition of TiH_2 paste for porous Ti scaffolds with tailored porous structures and mechanical properties, Mater. Chem. Phys., 176 (2016) 104-109.
[8] B.M. Patterson, J.P. Escobedo-Diaz, D. Dennis-Koller, E. Cerreta, Dimensional quantification of embedded voids or objects in three dimensions using x-ray tomography, Microsc. Microanal., 18 (2012) 390-398.
[9] Y.J. Liu, S.J. Li, H.L. Wang, W.T. Hou, Y.L. Hao, R. Yang, T.B. Sercombe, L.C. Zhang, Microstructure, defects and mechanical behavior of beta-type titanium, porous structures manufactured by electron beam melting and selective laser melting, Acta Mater. 113 (2016) 56-67.
[10] H. Liu, G. Yao, Z. Cao, Energy absorption of aluminum foam-filled tubes under quasi-static axial loading, Light Metals (2012) 515-520.
[11] Y. Liao, G. Qiu, Y. Yang, X. Lv, C. Bai, Preparation and compressive properties of magnesium foam, Rare Metal Mat. Eng., 45 (2016) 2498-2502.